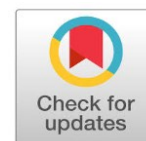




Original Research Article

**Fabrication, characterization and antibacterial properties of Ag<sub>2</sub>O QDs in molecular sieve matrix synthesized from rice husk silica at room temperature**



Roshanak Dadvand<sup>a</sup>, Afshin Pourahmad<sup>a,\*</sup>, Leila Asadpour<sup>b</sup>

<sup>a</sup> Department of Chemistry, Rasht Branch, Islamic Azad University, Rasht, Iran

<sup>b</sup> Department of Microbiology, Rasht Branch, Islamic Azad University, Rasht, Iran

**ARTICLE INFORMATION**

Received: 18 July 2019

Received in revised: 10 September 2019

Accepted: 2 October 2019

Available online: 31 December 2019

DOI: [10.22034/ajgc.2020.100452](https://doi.org/10.22034/ajgc.2020.100452)

**KEYWORDS**

Nanocomposite

Silver oxide

Rice husk

Molecular sieve

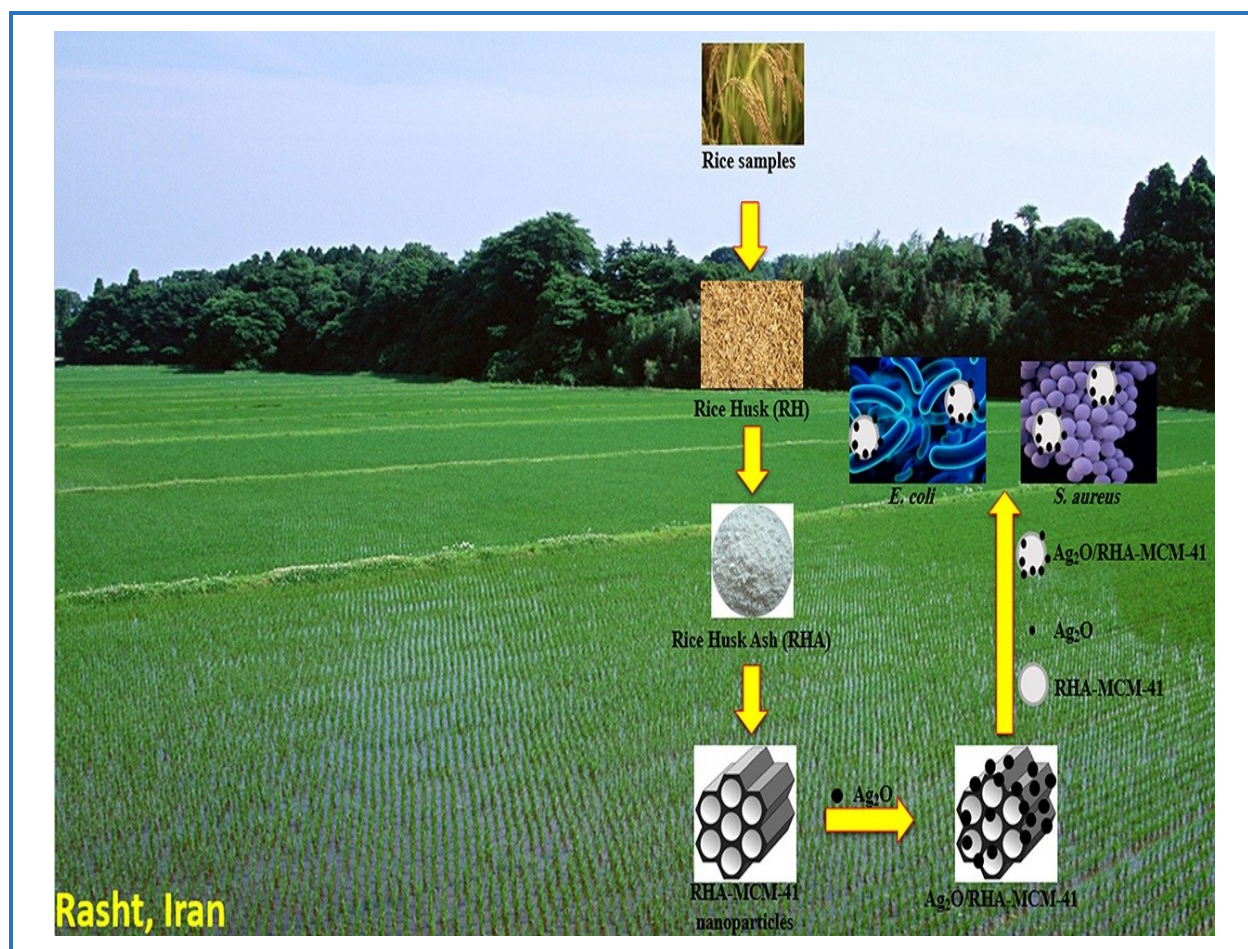
Antimicrobial

**ABSTRACT**

In this work, mesoporous MCM-41 nanoparticles (MCM-41NPs) were synthesized using the rice husk ash (RHA), as the silica source at room temperature. Ag<sub>2</sub>O quantum dots were prepared using a chemical method in matrix nanoparticles, and used as an antibacterial material. Bactericidal activity of the nanomaterials was investigated against *E. coli* and *S. aureus* bacteria. The synthesized materials were characterized using X-ray diffraction (XRD), scanning electron microscope (SEM), Fourier transform infrared spectroscopy (FT-IR), and transmission electron microscope (TEM). The minimum concentrations of nanocomposite to inhibit the growth of *E. coli* and *S. aureus* strains were 12.5 µg/mL. The Ag<sub>2</sub>O quantum dots indicated acceptable antimicrobial properties, with an average diameter of 16 nm.

© 2020 by SPC (Sami Publishing Company), Asian Journal of Green Chemistry, Reproduction is permitted for noncommercial purposes.

## Graphical Abstract



## Introduction

Antimicrobial materials play an important role in medicine, different industry, water aseptis, and substance packaging [1, 2]. Materials in the nanosize are one of the novel antimicrobial agents. *In vitro* and *in vivo*, animal models have shown the effectiveness of these nanostructures in treating infectious diseases, and the ones caused by antibiotic resistance bacteria [3].

Rice husk containing abundant SiO<sub>2</sub>, generally used in the preparation of zeolite. It is a natural substance, which has a low charge and reduces the process toxicity.

MCM-41 physical properties, such as controllable pore size and volume, and high surface area, permit them to be used as catalyst substance, adsorbents, and one of the most attractive supports for metal oxide or metal nanostructures [4, 5]. Ag<sub>2</sub>O, as a *p*-type semiconductor with narrow band gap (1.46 eV), has been studied as a necessary substance in photocatalysis [6], and antimicrobial materials [1]. Although the antimicrobial activities of the silver nanomaterials have been studied, the mechanism is not clear yet. It is known that the silver nanomaterials could expunge bacteria system,

inhibiting growth of bacteria by release silver ions and generating reactive oxygen species [1–7]. Different methods have been applied for preparation of the silver oxide nanostructures with several morphologies. In this work, we successfully synthesized MCM-41NPs using the RHA as a silica source by a simple and green method at room temperature. The reports revealed that, up to now there has been no reported on the synthesis of MCM-41NPs. So, the ultrafine  $\text{Ag}_2\text{O}$  (4 nm, determined by TEM) was prepared using a chemical method in RHA-MCM-41NPs ( $\text{Ag}_2\text{O}$ /RHA-MCM-41 nanocomposite (NC)), and evaluated as an antibacterial material.

## Experimental

### *Materials and methods*

The RH was gathered at a local rice milling plant in the State of Guilan, Iran. Cetyltrimethylammonium bromide (CTAB), hydrochloric acid, nitric acid, ethylamine, copper (II) acetate, and sodium hydroxide were bought from Merck.

### *Preparation of RHA and sodium silicate*

About 15 g of clean RH was mixed with 375 mL of  $1.0 \text{ mol/L}^{-1} \text{HNO}_3$  at  $25^\circ\text{C}$  for 24 h. After that the prepared sample was washed with distilled water for constant pH, dried at  $100^\circ\text{C}$  for 12 h and calcined in a furnace at  $600^\circ\text{C}$  for 5 h. The synthesized sample (RHA) was white [8]. About 1.5 g of RHA was mixed with 87.5 mL of  $2 \text{ mol/L}^{-1}$  sodium hydroxide then stirred for 24 h at  $25^\circ\text{C}$ , to solve the silica. The obtained sodium silicate was used as the  $\text{SiO}_2$  source for the synthesis of MCM-41NPs.

### *Synthesis of RHA-MCM-41NPs*

The MCM-41NPs was prepared by a room temperature method with some turnover in the described process in the literature [5]. Sodium silicate and hexadecyltrimethylammonium bromide (HDTMABr, BDH) as a source of silicon and a surfactant template were used for synthesis of MCM-41NPs matrix, respectively. The reacting mixture had molar composition of:

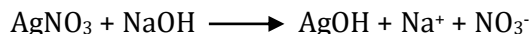


EA stands for ethylamine.

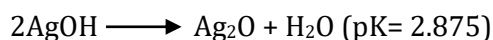
### *Preparation of $\text{Ag}_2\text{O}$ /RHA-MCM-41NC*

$\text{Ag}_2\text{O}$  NP was prepared by a wet chemical method 1 g of RHA-MCM-41NPs was added to 80 mL of 0.005 M silver nitrate ( $\text{AgNO}_3$ ) solution and was heated to  $60^\circ\text{C}$ . 20 mL of a 0.025 M NaOH solution

was added drop-wise to above solution and stirred until the solution changing to a gray-yellow colloidal suspension. The reaction mechanism was:



The intermediate AgOH is thermodynamically unstable, and finally convert to Ag<sub>2</sub>O compound through the following process:



The reaction was completed at 65 °C for 2 h. The solid material was gathered and Ag<sub>2</sub>O/RHA-MCM-41NC dried at room temperature.

#### *Test bacteria and growth conditions*

In this study, clinical isolates of *Staphylococcus aureus* (*S. aureus*) and *Escherichia coli* (*E. coli*) were applied to test the antibacterial properties of Ag<sub>2</sub>O/RHA-MCM-41NC. To prepare a fresh culture of test bacteria, 1 g of nutrient broth powder was mixed in 50 mL distilled water by moderately shaking. The mixture was sterilized in an autoclave and permitted to cool. Bacterial strains were moved into the medium with 37 °C and incubated for 24 h.

#### *Antibacterial activity assay*

Approximately 25 mL of autoclaved, cooled Mueller–Hinton agar media was poured into the sterilized petri dishes. Antimicrobial tests were prepared by picking colonies from 24 h old broth cultures. From each culture, 1 mL was diluted with Mueller–Hinton broth medium to 1.5×10<sup>8</sup> CFU/mL. Then, 100 µL of each dilution was transferred to the Mueller–Hinton agar medium, and the bacterial lawns were prepared using sterile cotton swabs. The sensitivity of the test bacteria to common antibiotics and the antimicrobial activity of the synthesized compound were evaluated using the agar disk diffusion method. Standard antibiotic impregnated disks (Mast Group, Bootle, and Merseyside, UK) and disk containing of Ag<sub>2</sub>O/RHA-MCM-41NC with 6 mm diameter were located in each plate. One disk in a plate was installed as a negative control by combining with sterile saline solution at 37 °C for 24 h. To measure the minimum inhibitory concentration (MIC) of Ag<sub>2</sub>O/RHA-MCM-41NC, 3 mg was moved to a test tube and scattered in 1 mL of 0.9% sterile saline solution. The tube was disturbed on an orbital shaker at 650 rpm at 37 °C for 3 h. After that, the tube was separated for 10 min at 100 rpm, and a twofold serial dilution of supernatant was prepared using a sterile saline solution. The disks were medicated with each bacterial dilution positioned in the center of the plates with a meadow culture of test bacteria and incubated for 24 h at 37 °C.

## Results and Discussion

The powder XRD pattern of the rice husk ash showed very broad peak at the range of  $2\theta = 22.6\text{--}23.4^\circ$  that could be related to the amorphous nature of the  $\text{SiO}_2$  [1–9]. The XRD pattern of RHA-MCM-41 and  $\text{Ag}_2\text{O}$ /RHA-MCM-41NC are indicated in Figure 1. Figure 1a showed low angle XRD patterns of the synthesized samples.

The diffraction angle at  $2\theta = 2.55^\circ$  corresponds to long-range ordered hexagonal structure from MCM-41 matrix [4, 10]. Synthesis of  $\text{Ag}_2\text{O}$  quantum dots in the channels of RHA-MCM-41 matrix leads to the loss of ordering structure resulting in the decrease in intensity reflection  $2\theta = 2.55^\circ$ . Decrease in the intensity could be related to the pore filling effects, reducing the dispersion contrast between the pores and the framework of the RHA-MCM-41 sample. Figure 1b depicted a high angle XRD pattern ( $2\theta = 30\text{--}80^\circ$ ) of samples and further displayed presence of  $\text{Ag}_2\text{O}$ . The peak rises at  $2\theta = 32.28^\circ$ ,  $38.01^\circ$ ,  $54.93^\circ$ ,  $66.81^\circ$  and  $69.93^\circ$  corresponds to (1 1 1), (2 0 0), (2 2 0), (3 1 1), and (2 2 2) planes of silver oxide lattice. No peak was observed between  $10^\circ$  and  $80^\circ$  for matrix (not shown) [4]. In contrast with the standard diffraction patterns for  $\text{Ag}_2\text{O}$  (JCPDS 12-0793), the diffraction peaks at  $2\theta$  equal to  $32.28^\circ$ ,  $38.01^\circ$ ,  $54.93^\circ$ ,  $66.81^\circ$ , and  $69.93^\circ$  for  $\text{Ag}_2\text{O}$ /RHA-MCM-41 nanocomposites are assigned to that of cubic  $\text{Ag}_2\text{O}$  crystals [11]. The average crystallite sizes of RHA-MCM-41 and  $\text{Ag}_2\text{O}$  that calculated using the Scherrer's equation was 90 and 6 nm, respectively. All the  $\text{Ag}_2\text{O}$ /RHA-MCM-41 samples had relatively the same crystalline sizes, showing that the dispersion of  $\text{Ag}_2\text{O}$  quantum dots on the RHA-MCM-41NP surface has no obvious influence on the crystallite size.

The FT-IR spectra of RHA, RHA-MCM-41NPs and  $\text{Ag}_2\text{O}$ /RHA-MCM-41NC were researched in the range of  $400\text{--}4000\text{ cm}^{-1}$ . The broad band around  $3432\text{--}3469\text{ cm}^{-1}$  can be related to stretching vibration O-H groups in MCM-41 samples [12]. The band at  $1634\text{--}1645\text{ cm}^{-1}$  can be assigned to the bending vibration of  $\text{H}_2\text{O}$  trapped within the  $\text{SiO}_2$  matrix. The band at  $1074\text{--}1100\text{ cm}^{-1}$  was attributed to stretching vibration of Si-O-Si in the structure of siloxane. The band at  $466\text{ cm}^{-1}$  is due to Si-O-Si bending vibrations. The band at  $806$  and  $639\text{ cm}^{-1}$  can be assigned to stretching vibrations of Si-OH and Ag-O-Ag, respectively [13]. The observed vibrational band at low frequency regions demonstrated the formation of  $\text{Ag}_2\text{O}$  quantum dots.

The morphology of the  $\text{Ag}_2\text{O}$ /RHA-MCM-41NC also was investigated by TEM (Figure 2). As can be seen in Figure 2,  $\text{Ag}_2\text{O}$  nanoparticles of  $\sim 4\text{ nm}$  were formed and stuck to the surface of the RHA-MCM-41NPs. No free  $\text{Ag}_2\text{O}$  nanoparticle was found.

The nitrogen absorption/desorption isotherms (Figure 3a) for the  $\text{Ag}_2\text{O}$ /RHA-MCM-41 nanocomposite correspond to type IV isotherms with a steep increase in the nitrogen uptake around  $P/P_0=0.37$  [14]. The Barrett-Joyner-Halenda (BJH) model (Figure 3b) and BET results showed the pore size  $2.5\text{ nm}$  and the specific surface  $450\text{ m}^2/\text{g}$  for  $\text{Ag}_2\text{O}$ /RHA-MCM-41NC, respectively.



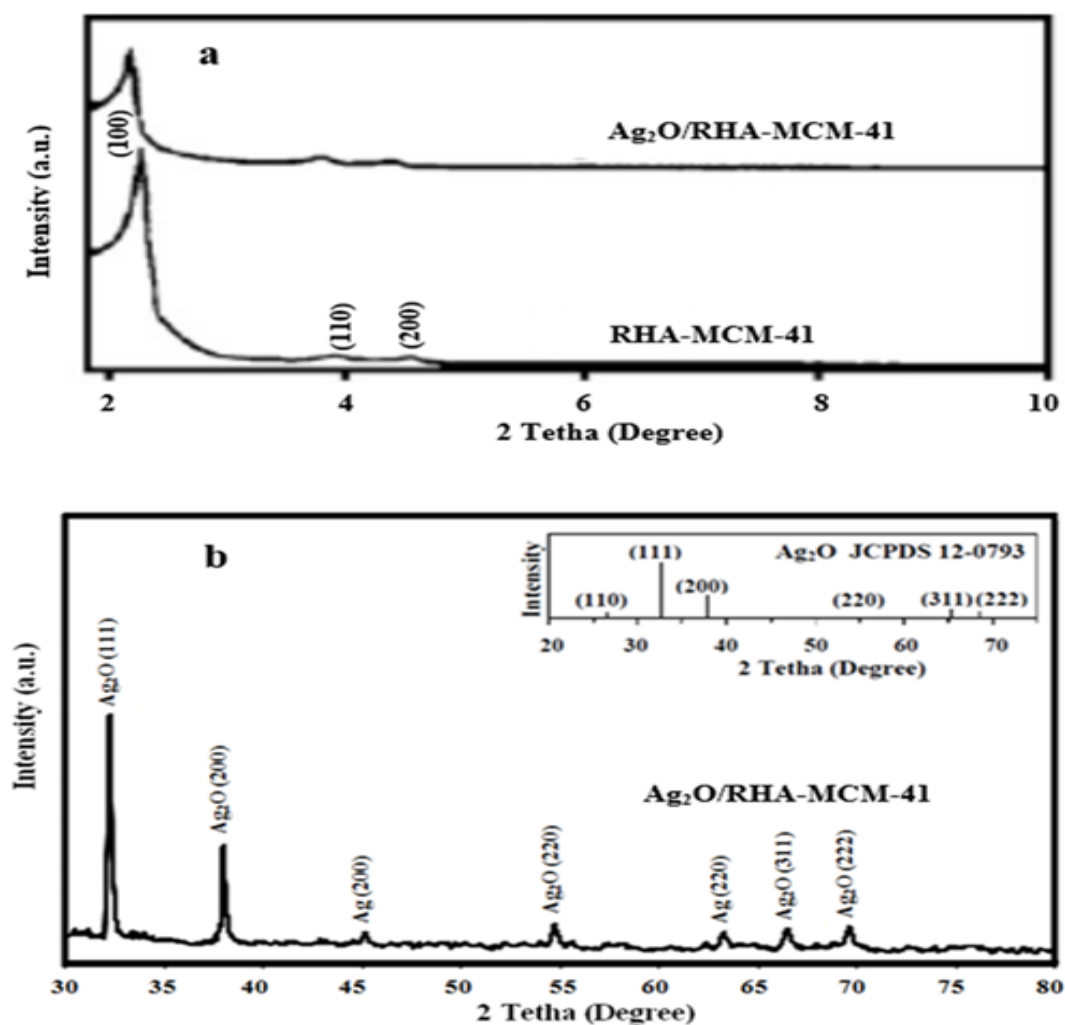


**Figure 1.** XRD patterns of RHA-MCM-41NPs and Ag<sub>2</sub>O/RHA-MCM-41NC in range of a)  $2\theta = 2\text{--}10^\circ$  and b)  $2\theta = 30\text{--}80^\circ$ . The insert shows XRD patterns of Ag<sub>2</sub>O nanostructures

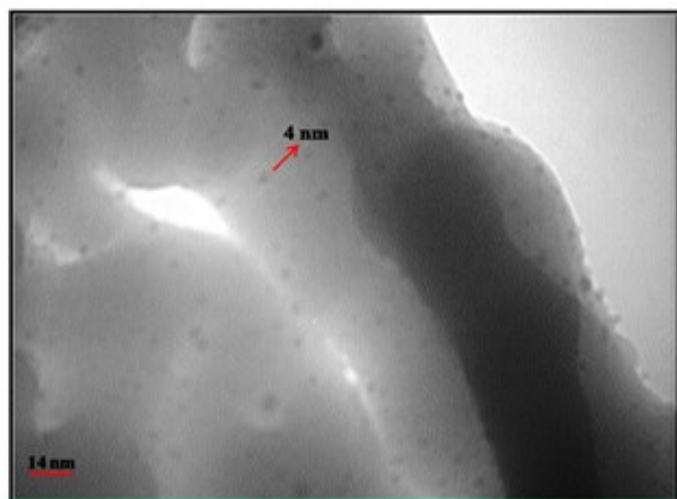


**Figure 2.** TEM image of the Ag<sub>2</sub>O/RHA-MCM-41NC

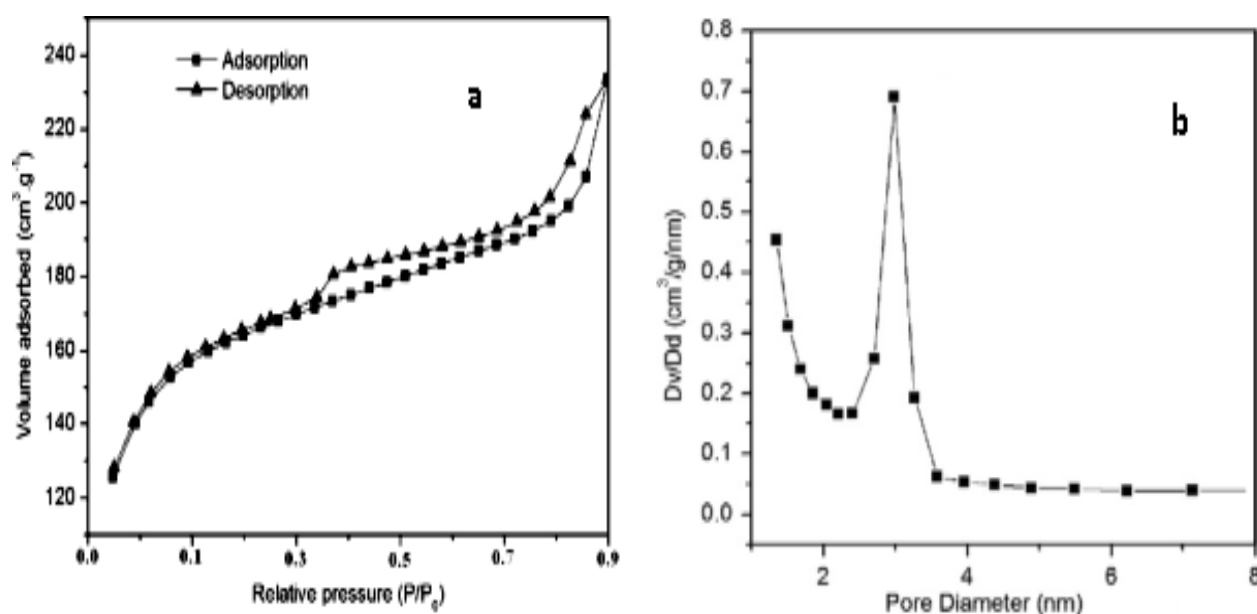


**Figure 3.** Nitrogen adsorption-desorption isotherms a) and pore size distribution of the mesoporous micropores b) of Ag<sub>2</sub>O/RHA-MCM-41NC

The MIC of antibacterial samples was measured by the lowest concentration samples that entirely prevented visible growth, as advised by the naked eye, disassembling a single colony or a thin haze into the area of the inseeded spot. This test was repeated (twice) and the results were found to be at the same range. The minimum inhibitory concentration values against *E. coli* and *S. aureus* of the samples were 100 µg/mL for RHA-MCM-41NP, 30 µg/mL for Ag<sub>2</sub>O NPs, and 12.5 µg/mL for Ag<sub>2</sub>O/RHA-MCM-41NC. The disk ability tests are depicted in Table 1 and Table 2. The results showed that, the RHA-MCM-41NPs had hardly any antibacterial properties against the *E. coli* and *S. aureus*. The diameter of inhibition zone and the amount of swelling from the edge of each disk in the agar plate were determined in mm. The test was performed at least three times for each treated sample. No antibacterial activity of RHA-MCM-41NPs was observed. Ag<sub>2</sub>O/RHA-MCM-41NC illustrated good antibacterial activity, with an average diameter of 16.0 mm, and Ag<sub>2</sub>O NPs showed antibacterial activity, with an average diameter of 11 mm.

**Table 1.** The diameter of inhibition zone from synthesized samples

Sample	Initial diameter (mm)	Final inhibition zone diameter (mm)	Diffusion (mm)
RHA-MCM-41 (100 µg/mL)	6.0 ± 0.0	6.2 ± 0.1	0.2 ± 0.1 <sup>a</sup>
Ag <sub>2</sub> O NPs (30 µg/mL)	6.0 ± 0.0	11 ± 0.1	5.0 ± 0.1
Ag <sub>2</sub> O/RHA-MCM-41(12.5 µg/mL)	6.0 ± 0.0	16.0 ± 0.2	10.0 ± 0.2

<sup>a</sup> The values are means of triplicate with ± SD

**Table 2.** Antibacterial properties of Ag<sub>2</sub>O/RHA-MCM-41NC in comparing with standard antibiotics

Antibacterial agent	Diameter of zone of inhibition of <i>E. coli</i> (mm)	Diameter of zone of inhibition of <i>S. aureus</i> (mm)
Ag <sub>2</sub> O/RHA-MCM-41 (12.5 μg/mL)	16	16
Gentamicin (10 μg/mL)	23	30
Cefotaxime (30 μg/mL)	12	0
Amoxicillin (25 μg/mL)	0	16
Cefepime (30 μg/mL)	0	14
Tetracycline (30 μg/mL)	14	0
Ampicillin (10 μg/mL)	0	0

Silver nanostructures are inorganic nanostructures used as antibacterial agents [15]. Antibacterial application of the silver additives is widely benefitted in textiles, coating-based usages, and the various injection molded plastic products [16]. Ag nanostructures show a high antibacterial activity comparable with its ionic form [17]. Ag<sub>2</sub>O nanostructures revealed great antibacterial activity [18]. Metal oxide nanomaterials might be considered as a novel alternative to the most antibiotics [18]. Researchers demonstrated antibacterial efficacy of silver oxide nanostructures against *E. coli*. They proposed that when *E. coli* was exposed to these nanostructures, DNA lost its replication ability and the cell cycle halted at the G2/M phase owing to the DNA damage. Then the cell was affected by oxidative stress, and apoptosis was induced [19]. In our work, probably, Ag<sup>+</sup> ions released from the surface of Ag<sub>2</sub>O NPs are responsible for their antibacterial activity.

The results exhibited that incorporation of the Ag<sub>2</sub>O in RHA-MCM-41 increased the antibacterial activity with respect to other supports [18–21].

## Conclusions

In this study, amorphous RHA was produced under controlled burning conditions and was utilized as an alternative cheap SiO<sub>2</sub> source for the synthesis of MCM-41 nanoparticles at room temperature. Both the produced RHAs and the synthesized mesoporous materials were characterized using several analytical techniques including, XRD, FT-IR, TEM, and SEM. The FT-IR and XRD data revealed that, the highly pure MCM-41NPs was successfully prepared from rice husk ash. Ag<sub>2</sub>O quantum dots were synthesized using a chemical method in matrix nanoparticles, and estimated as an antibacterial material. The results of the TEM analysis indicated that, the Ag<sub>2</sub>O nanoparticles (with the particle size



of ~ 4 nm) were formed and stuck to the surface of the RHA-MCM-41NPs. Ag<sub>2</sub>O/RHA-MCM-41NC also depicted high antibacterial activity against drug-resistant *E. coli* and *S. aureus* strains.

### Acknowledgements

The authors would like to acknowledge the, Islamic Azad University, Rasht Branch for its financial supports.

### Disclosure Statement

No potential conflict of interest was reported by the authors.

### References

- [1]. Ziksari M., Pourahmad A. *Indian J. Chem. Sect. A*, 2016, **55A**:1347
- [2]. Levy S.B., Marshall B. *Nat. Med.*, 2004, **10**:S122
- [3]. Salata O.V. *Rev. J. Nanobiotechnol.*, 2004, **2**:3
- [4]. Pourahmad A. *Synth. React. Inorg. Met. Org. Chem.*, 2015, **45**:1080
- [5]. Pourahmad A. *Spectrochim. Acta A*, 2013, **103**:193
- [6]. Pourahmad A. *Arabian J. Chem.*, 2014, **7**:788
- [7]. Kittler S., Greulich C., Diendorf J., Koller M., Epple M. *Chem. Mater.*, 2010, **22**:4548
- [8]. Srivastava V.C., Mall I.D., Mishra I.M. *J. Hazard. Mater.*, 2006, **134**:257
- [9]. Thuadaj N., Nuntiya A. *Chiang Mai. J. Sci.*, 2008, **35**:206
- [10]. Beck J.S., Vartuli J.C., Roth W.J., Leonowicz M.E., Kresge C.T., Schmitt K.D., Chu C.T.W., Olson D.H., Sheppard E.W. *J. Am. Chem. Soc.*, 1992, **114**:10834
- [11]. Sullivan K.T., Wu C., Piekiet N.W., Gaskell K., Zachariah M.R. *Combust. Flame*, 2013, **160**:438
- [12]. Ahmed A.E., Adam F. *Micropor. Mesopor. Mater.*, 2007, **103**:284
- [13]. Endud S., Wong K.L. *Micropor. Mesopor. Mater.*, 2007, **101**:256
- [14]. Yang H., Coombs N., Ozin G.A. *Nature*, 1997, **386**:692
- [15]. Zinjarde S. *Chronicles Young Sci.*, 2012, **3**:1
- [16]. Egger S., Lehmann R.P., Height M.J., Loessner M.J., Schuppler M. *Appl. Environ. Microbiol.*, 2009, **75**:2973
- [17]. Jo Y.K., Kim B.H., Jung G. *Plant Dis.*, 2009, **93**:1037
- [18]. Allahverdiyev A.M., Abamor E.S., Bagirova M., Rafailovich M. *Future Microbiol.*, 2011, **6**:933
- [19]. Sondi I., Salopek-Sondi B.J. *Coll. Interface Sci.*, 2004, **275**:177
- [20]. Chen C.C., Wu H.H., Huang H.Y., Liu C.W. Chen Y.N. *Int. J. Environ. Res. Public Health.*, 2016, **13**:99
- [21]. Ni S., Li X., Yang P., Ni S., Hong F., Webster T.J. *Mater. Sci. Eng. C.*, 2016, **58**:700

**How to cite this manuscript:** Roshanak Dadvand, Afshin Pourahmad\*, Leila Asadpour. Fabrication, characterization and antibacterial properties of Ag<sub>2</sub>O QDs in molecular sieve matrix synthesized from rice husk silica at room temperature. *Asian Journal of Green Chemistry*, 4(4) 2020, 387-396. DOI: [10.22034/ajgc.2020.100452](https://doi.org/10.22034/ajgc.2020.100452)